

## Individual differences in the mechanistic control of the dopaminergic midbrain

Lydia Hellrung<sup>1\*</sup>, Matthias Kirschner<sup>2,3</sup>, James Sulzer<sup>4</sup>, Ronald Sladky<sup>2</sup>, Frank Scharnowski<sup>2</sup>,  
Marcus Herdener<sup>2</sup>, Philippe N. Tobler<sup>1</sup>

<sup>1</sup> Laboratory for Social and Neural Systems Research, Department of Economics, University of Zurich,  
Switzerland, University of Zurich, Zurich, Switzerland

<sup>2</sup> Center for Addictive Disorders, Psychiatric University Hospital, University of Zurich, Zurich,  
Switzerland

<sup>3</sup> Montreal Neurological Institute, McGill University, Montreal, Canada

<sup>4</sup> Department of Mechanical Engineering, University of Texas at Austin, Austin, USA

### **Corresponding author:**

Lydia Hellrung, Laboratory for Social and Neural Systems Research, Department of Economics,  
University of Zurich, Blümlisalpstrasse 10, 8006 Zurich, Switzerland; E-mail:  
[lydia.hellrung@econ.uzh.ch](mailto:lydia.hellrung@econ.uzh.ch)

## Abstract

The dopaminergic midbrain is associated with elementary brain functions, such as reward processing, reinforcement learning, motivation and decision-making that are often disturbed in neuropsychiatric disease. Previous research has shown that activity in the dopaminergic midbrain can be endogenously modulated via neurofeedback, suggesting potential for non-pharmacological interventions. However, the robustness of endogenous modulation, a requirement for clinical translation, is unclear. Here, we used non-invasive modulation of the dopaminergic midbrain activity by real-time neurofeedback to examine how self-modulation capability affects transfer and correlated activation across the brain. In addition, to further elucidate potential mechanisms underlying successful self-regulation, we studied individual prediction error coding during neurofeedback training, and, during a completely independent monetary incentive delay (MID) task, individual reward sensitivity. Fifty-nine participants underwent neurofeedback training either in a veridical or inverted feedback group. Post-training activity within the cognitive control network was increased only in those individuals with successful self-regulation of the dopaminergic midbrain during neurofeedback training. Successful learning to regulate was accompanied by decreasing prefrontal prediction error signals and increased prefrontal reward sensitivity in the MID task. Our findings suggest that the cognitive control network contributes to successful transfer of the capability to upregulate the dopaminergic midbrain. The link of dopaminergic self-regulation with individual differences in prefrontal prediction error and reward sensitivity indicates that reinforcement learning contributes to successful top-down control of the midbrain. Our findings therefore provide new insights in the cognitive control of dopaminergic midbrain activity and pave the way to improving neurofeedback training in neuropsychiatric patients.

**Keywords:** real-time fMRI, neurofeedback, dopaminergic midbrain, substantia nigra, ventral tegmental area, dorsolateral prefrontal cortex, self-regulation, prediction error, reinforcement learning

## 1 1 Introduction

2 The dopaminergic midbrain, including the ventral tegmental area (VTA) and substantia nigra (SN), plays  
3 a crucial role in reward processing, reinforcement learning (Schultz, 2016, 1998; Tobler et al., 2007),  
4 motivation (Bromberg-Martin et al., 2010; Wise, 2004), and decision-making (Friston et al., 2014).  
5 Dysfunctions of the reward system have far-reaching consequences and are associated with the  
6 development of several severe psychiatric disease such as addiction (Huys et al., 2014) and  
7 schizophrenia (Deserno et al., 2016; Maia and Frank, 2017). Despite decades of extensive neuroscience  
8 and imaging studies which have contributed to an impressive body of knowledge of normal and  
9 abnormal reward system function, the neural mechanisms controlling midbrain activity are still not  
10 fully understood (Meder et al., 2019). One key issue that has received increasing attention over the  
11 last years is whether humans are able to cognitively control brain activity within the reward system.  
12 Although the mechanisms remained unclear, it has already been shown that both healthy controls  
13 (MacInnes et al., 2016; Sulzer et al., 2013b), and patients with cocaine addiction (Kirschner et al.,  
14 2018c) can learn to regulate SN/VTA activity during real-time functional magnetic resonance imaging  
15 (rt-fMRI) neurofeedback training. Yet, only little or no behavioral changes or increases in neural activity  
16 have been found so far to transfer beyond neurofeedback training, even though transfer, i.e., the  
17 ability to regulate activity also after training and without feedback is critical for clinical applications in  
18 disorders with reward system dysfunctions (Klein et al., 2019). The question therefore arises how  
19 individuals with successful transfer effects differ from individuals without transfer effects and what  
20 mechanisms underpin transfer effects. We narrowed this gap by combining data from two previous rt-  
21 fMRI studies (Kirschner et al., 2018c; Sulzer et al., 2013b) and pursuing three aims.

22 (1) Our first goal was to characterize individual differences in transfer effects between  
23 'regulators' and 'non-regulators' in the context of SN/VTA self-regulation. Individual differences in  
24 regulation success and high variability of transfer effects arises also in other neurofeedback modalities  
25 such as electroencephalography (EEG) and are often neglected (Alkoby et al., 2018). For rt-fMRI

26 neurofeedback control, neural activity in the cognitive (or executive) control network may play an  
27 important role especially when performing a demanding task such as imagery (Sitaram et al., 2016).  
28 Therefore, and based on the known direct and indirect connections between prefrontal cortex and  
29 SN/VTA (Frankle et al., 2006; Gao et al., 2007; Sesack et al., 2003; Wu et al., 2013) we hypothesize that  
30 successful transfer of SN/VTA regulation is associated with activation in brain regions that are part of  
31 the cognitive (executive) control network, especially prefrontal areas.

32 (2) Our second goal was to determine whether mechanisms of (operant) associative learning  
33 can be used to explain neurofeedback training. In the associative learning framework of neurofeedback  
34 (Birbaumer et al., 2013; Sitaram et al., 2016), the chosen mental strategy is reinforced in proportion  
35 to the sign and magnitude of the feedback. If the feedback signal increases, reflecting a desired  
36 increase in brain activity within the target region, participants receive more reward than predicted  
37 corresponding to a positive prediction error. As a consequence, they would be more likely to repeat  
38 the strategy, expect higher feedback next time and gradually learn how to keep the feedback signal  
39 high. Accordingly, in regulators the size of the prediction error should gradually decrease as the  
40 expected feedback increasingly converges with the actual feedback. In contrast, for non-regulators and  
41 participants in a control group receiving unrelated or unstable feedback, the prediction errors would  
42 remain large and variable because these participants cannot learn any association between mental  
43 strategies and feedback. These straightforward implications of current theorizing about the  
44 mechanisms underlying neurofeedback remained largely untested (for a simulation study on the  
45 temporal dynamics of feedback: Oblak and colleagues (2017); for the correlation of BOLD with signal  
46 increase ('success') and decrease ('failure') during regulation: Radua and colleagues (2018)). Here, we  
47 directly investigate the prediction error mechanism in regions that control the SN/VTA, which itself has  
48 been traditionally associated with the coding of reward prediction errors (Schultz, 2016). Specifically,  
49 we hypothesize that decreasing prediction error signals during neurofeedback learning are associated  
50 with successful self-regulation and transfer effects.

51 (3) Our third aim was to identify individual differences in the ability to regulate the midbrain  
52 to general characteristics of the reward system, hoping to further distinguish regulators from non-  
53 regulators. Thus, we asked whether successful neurofeedback training (as measured by transfer  
54 effects) taps into general properties of the reward system. Given that adaptive reward processing  
55 characterizes the SN/VTA (Schultz, 1998; Tobler et al., 2005) we used a variant of the monetary  
56 incentive delay (MID) task that captures differences in adaptive reward sensitivity between clinical and  
57 non-clinical populations (Kirschner et al., 2018a). Using this task, we tested the hypothesis that reward  
58 processing in regions that may control the dopaminergic midbrain is related to successful SN/VTA self-  
59 regulation.

60 In sum, to study individual differences in capability to gain control of the SN/VTA we used rt-  
61 fMRI neurofeedback training in healthy participants receiving either real feedback (veridical group) or  
62 inverted feedback (control group). We quantified the individual degree of successful transfer by  
63 comparing the individual post-training versus pre-training self-regulation capabilities. Moreover, we  
64 related individual differences in reward sensitivity in separately measured SN/VTA self-regulation  
65 success.

## 66 2 Methods

### 67 2.1 Participants

68 Fifty-nine right-handed participants (45 males, average age  $28.25 \pm 5.25$  years) underwent  
69 neurofeedback training. We analysed data from two independent projects, which used highly similar  
70 rt-fMRI paradigms, rt-fMRI software and scanner hardware. The first dataset (Sulzer et al., 2013b)  
71 comprised male participants, randomly assigned to one of two groups. The experimental group  
72 received veridical neurofeedback ( $N = 15$ ), the control group received inverted neurofeedback ( $N = 16$ )  
73 as training signal. The second dataset (Kirschner et al., 2018c) comprised the healthy control  
74 participants ( $N=28$ , 14 males) of a project investigating also cocaine users (these data are not  
75 presented here). This group received veridical neurofeedback. A subset of the participants in the

76 second dataset (N=25) also performed a variant of the monetary incentive delay (MID) task (Kirschner  
77 et al., 2018a). All participants provided written informed-consent and have been compensated for  
78 their participation. The Zurich cantonal ethics committee approved these studies in accordance with  
79 the Human Subjects Guidelines of the Declaration of Helsinki.

80 **2.2 Experimental setup and neuroimaging**

81 All participants underwent neuroimaging in a Philips Achieva 3 Tesla magnetic resonance (MR) scanner  
82 using an eight channel SENSE head coil (Philips, Best, The Netherlands) either at the Laboratory for  
83 Social and Neural Systems Research Zurich (SNS Lab, Study 1) or the MR Center of the Psychiatric  
84 Hospital of the University of Zurich (Study 2). First, we acquired anatomical images (Study1: gradient  
85 echo T1-weighted sequence in 301 sagittal plane slices of  $250 \times 250 \text{ mm}^2$  resulting in  $1.1 \text{ mm}^3$  voxels;  
86 Study2: spin-echo T2-weighted sequence with 70 sagittal plane slices of  $230 \times 184 \text{ mm}^2$  resulting in  
87  $0.57 \times 0.72 \times 2 \text{ mm}^3$  voxel size) prior to neurofeedback training and loaded them into BrainVoyager QX  
88 v2.3 (Brain Innovation, Maastricht, The Netherlands) to identify SN/VTA as target region (see 2.4 for  
89 details). To acquire functional data, we used 27 ascending transversal slices in a gradient echo T2\*-  
90 weighted whole brain echo-planar image sequence in both studies. The in-plane resolution was  $2 \times 2$   
91  $\text{mm}^2$ , 3 mm slice thickness and 1.1 mm gap width over a field of view of  $220 \times 220 \text{ mm}^2$ , a TR/TE of  
92 2000/35 ms and a flip angle of 82°. Slices were aligned with the anterior–posterior commissure and  
93 then tilted by 15°. Functional images were converted from Philips par/rec data format to ANALYZE and  
94 exported in real-time to the external analysis computer via the DRIN software library provided by  
95 Philips. This external computer ran Turbo BrainVoyager v3.0 (TBV – Brain Innovation, Maastricht, The  
96 Netherlands) to extract the BOLD signal from the images and calculate the neural activation for the  
97 feedback signal. The visual feedback signal was presented using custom-made software with Visual  
98 Studio 2008 (Microsoft, Redmond, WA, USA) through either a mirror mounted at the rear end of the  
99 scanner bore (Study 1) or through MR compatible goggles (Study 2).

100 **2.3 Neurofeedback paradigm**

101 The participants were instructed that their goal was to control a reward-related region-of-interest in  
102 their brains by imagining rewarding stimuli, actions, or events (note that we have previously shown  
103 that reward imagination activates SN/VTA with standard fMRI (Miyapuram et al., 2012)). Prior to  
104 scanning, we provided examples of such rewards, including palatable food items, motivating  
105 achievements, positive experiences with friends and family, favourite leisure activity or romantic  
106 imagery. We encouraged participants to use these different rewards as potential strategies for  
107 upregulating reward-related activity (during the cue ‘Happy Time!’, here referred to as  
108 IMAGINE\_REWARD condition), which was fed back visually with a smiley vertically translating  
109 proportional to the SN/VTA BOLD signal (see below). In contrast, during the cue ‘Rest’ (here referred  
110 to as REST condition), participants were asked to perform neutral imagery, such as mental calculation  
111 to reduce reward-related activity. Prior to training, participants were familiarized with the 5s delay of  
112 the hemodynamic response affecting the display of the feedback and were asked not to move or  
113 change their breathing during the neurofeedback training.

114 Each neurofeedback session comprised: a pre-training imagery baseline run without any  
115 feedback, three (Study 1) or two (Study 2) training runs during which neurofeedback was presented  
116 (as Study 2 also investigated patients, training was limited to two runs), and a transfer run (i.e., without  
117 feedback). Each of these runs comprised nine blocks of IMAGINE\_REWARD and REST conditions, each  
118 lasting 20 s. To determine the current level of the feedback signal we used the average of the last five  
119 volumes of the previous REST condition as reference value and employed a moving average of the  
120 previous three volumes to reduce noise. In the veridical feedback group, the smiley moved up with  
121 increasing percent signal change of SN/VTA BOLD signal and changed colour from red to yellow (Fig. 1  
122 A). In the inverted feedback group, the smiley moved up and turned yellow with a decreasing SN/VTA  
123 BOLD signal.

124

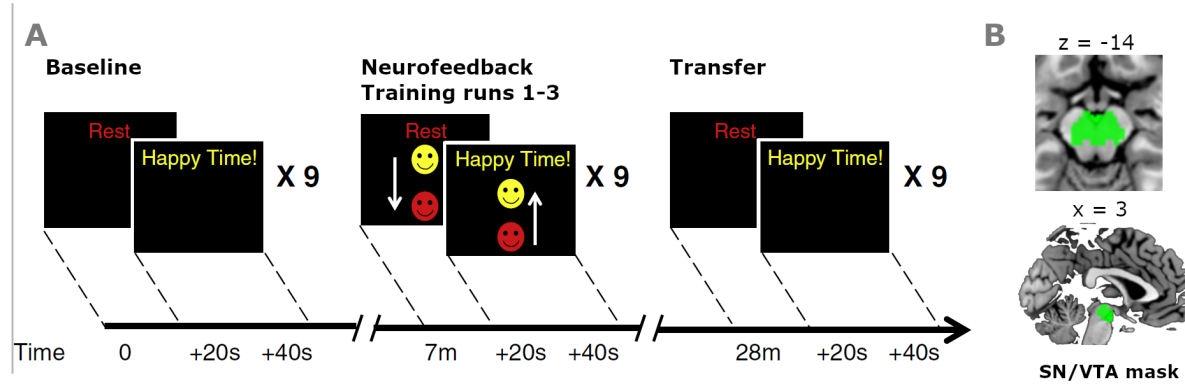


Figure 1 **Neurofeedback paradigm:** (A) All runs consisted of alternating blocks of REST and IMAGINE\_REWARD conditions, with each block lasting 20 s. The regulation conditions (REST, IMAGINE\_REWARD) were indicated by words ('Rest' or 'Happy Time!') and the feedback presented as moving smiley face during neurofeedback training runs. The preceding baseline and subsequent transfer runs comprised no feedback. The SN/VTA signal difference from these runs served to quantify the degree of regulation transfer (DORT) as  $(SN/VTA_{BOLD\{IMAGINE\_REWARD, Transfer\}} - SN/VTA_{BOLD\{REST, Transfer\}}) - (SN/VTA_{BOLD\{IMAGINE\_REWARD, Baseline\}} - SN/VTA_{BOLD\{REST, Baseline\}})$ . (B) Post-processed SN/VTA signal was extracted from the probabilistic atlas mask defined by Murty et al. (2014).

125 **2.4 Region-of-interest SN/VTA**

126 In both studies, the target region for neurofeedback, i.e. the substantia nigra (SN) and ventral  
127 tegmental area (VTA), was structurally identified using individual anatomical scans. Since the individual  
128 mask definition slightly differed between Study 1 and 2 (T1-weighted scans in Study 1 and T2-weighted  
129 scans in Study 2), we used an independent mask for our post-hoc analysis. By this, we can control for  
130 individual differences between experimenter ROI selection strategies, to avoid interpolation  
131 confounds due to warping by normalization and use a reliable seed region for functional connectivity  
132 analysis. The mask we are using here is a probabilistic mask of the SN and VTA as defined by (Murty et  
133 al., 2014), which is based on a large sample set (148 datasets) and available on  
134 <https://www.adcocklab.org/neuroimaging-tools> (download August 2018). Figure 1B illustrates this  
135 mask within the brain.

136 **2.5 Degree of regulation transfer (DORT)**

137 We assessed the effects of individual differences in performance to characterise participants in  
138 'regulators' and 'non-regulators'. The measure of successful self-regulation was defined as individual  
139 degree of regulation transfer (DORT), i.e. as the condition-specific SN/VTA signal difference between  
140 post-training (Transfer) and pre-training (Baseline) runs:

141  $DORT = (SN/VTA\_BOLD_{IMAGINE\_REWARD, Transfer} - SN/VTA\_BOLD_{REST, Transfer}) - (SN/VTA\_BOLD_{IMAGINE\_REWARD, Baseline} - SN/VTA\_BOLD_{REST, Baseline})$

142  
143 Thus, a positive DORT corresponds to a relative increase in post-training SN/VTA activity compared to  
144 pre-training SN/VTA activity for the contrast IMAGINE\_REWARD minus REST. Please note that in these  
145 two runs (pre-training baseline, post-training transfer) no neurofeedback was presented. Thus to  
146 achieve positive transfer effects participants had to apply what they had learned during training runs.

147 **DORT distributions:** To investigate potential group differences in DORT, we transferred the extracted  
148 data to R (R-project R3.4.1). Using an anova, we tested for differences of the mean between the three  
149 groups (i.e. the two groups receiving veridical feedback in Studies 1 and 2 and the control group  
150 receiving inverted feedback in Study 1).

151 **DORT in fMRI analysis:** The DORT measure served to investigate the individual differences in successful  
152 transfer at the whole brain level. In particular, we were interested to identify regions that were  
153 positively associated with DORT and thus potentially contribute to regulation of the SN/VTA. For this  
154 analysis, we entered mean centered individual DORT levels in all fMRI second level statistical models  
155 (see 2.8). We excluded SN/VTA from all analyses to avoid any circularity.

156 **Spatial specificity control analysis:** To bolster the spatial specificity of our analysis about dopaminergic  
157 midbrain regulation, we additionally performed an analysis using the directly neighbored brain region  
158 of the parahippocampus as control target ROI. This target area is also active during the self-regulation  
159 task since the participants perform memory-based strategies. We extracted this mask from the wfu  
160 atlas and performed the identical main effects analysis as described above. To compare the results  
161 between our target ROI SN/VTA and control ROI in parahippocampus, we performed a conjunction  
162 analysis between the resulting contrast images. This comparison revealed only two common areas  
163 within the cerebellum and the Temporal Gyrus. The limited commonalities between these two target  
164 ROI's, especially in striatal and prefrontal areas, indicate the spatial specificity of our findings using the  
165 SN/VTA as target region (see Supplemental Material Figure S4 and Table S8).

166 **2.6 MID Task**

167 In every trial of the MID task (Kirschner et al., 2018b, 2016; Simon et al., 2015) first one of three cues  
168 appeared (Fig. S1). One cue was associated with large reward (ranging from 0 to 2.00 CHF), one cue  
169 with small reward (0 to 0.40 CHF) and one cue with no reward. After a delay of 2.5 to 3 s, participants  
170 had to identify an outlier from three circles by pressing one of three buttons as quickly as possible.  
171 Depending on the cue, their response time and the correctness of the answer, participants gained an  
172 amount of money. Importantly, the use of large and small reward ranges enables investigation of  
173 individual differences not only in general reward sensitivity but also in how well the reward system  
174 adapts to different reward distributions, so-called adaptive reward coding (Kirschner et al., 2018a).

175 **2.7 MR Data pre-processing**

176 We despiked the functional data using AFNI (<http://afni.nimh.nih.gov/afni>). To account for differences  
177 in EPI slice acquisition times we employed temporal interpolation of the MR signal, shifting the signal  
178 of the misaligned slices to the first slice (Sladky et al., 2011) using FSL 5 (FMRIB Software Library,  
179 Analysis Group, FMRIB, Oxford, <http://fsl.fmrib.ox.ac.uk>). Furthermore, data were bias-field corrected  
180 using ANTs (<http://stnava.github.io/ANTs>), realigned using FSL 5, normalized to standard MNI space  
181 using ANTs in combination with a custom scanner-specific EPI-template resulting in a 1.5  
182 mm<sup>3</sup> isotropic resolution and finally smoothed with a 6 mm FWHM Gaussian kernel using FSL 5.

183 The spatial specificity control analyses (see Supplemental Material Figure S4 and Table S8)  
184 suggest that the data are not due to common physiological noise. To more directly account for noise,  
185 we additionally acquired physiological data in a subsample of participants. In the available subsample,  
186 neither changes in heart rate variability nor respiration were significantly correlated with VTA/SN  
187 activation during reward imagination (see details in Kirschner et al., 2018, Supplemental Material Table  
188 S1, Figure S1). Here, we also used an image-based correction to account for physiological artefacts in  
189 all participants. Since physiological artefacts are most prominently present in CSF and white matter  
190 due to the absence of BOLD effects, pulsations of the ventricles, and proximity to the large brain  
191 arteries (e.g., circle of Willis), we decided to use an established preprocessing procedure based on a

192 PCA approach (Sladky et al., 2013; Weissenbacher et al., 2009). Specifically, we calculated the global  
193 mean and the first 6 components of a temporal principal component analysis on the cerebrospinal  
194 fluid and white matter signal. These 6 components were used as noise regressors in the first level  
195 statistics (see 2.8) in addition to the 6 motion parameters. Along with the pre-processing of the fMRI  
196 data, the SN/VTA mask used as ROI for the analysis was resliced into the dimensions of the functional  
197 data using SPM 12 (v6906, <http://www.fil.ion.ucl.ac.uk/spm/software/spm12/>) within Matlab R2016b  
198 ([www.mathworks.com](http://www.mathworks.com)).

199 **2.8 MR Data analysis**

200 For all of the following analyses, we used the toolbox SPM 12 (v6906) within Matlab R2016b. All figures  
201 were created using bspmview v.20161108 (Spunt, 2016) and ggplot2 within R 3.4.1. All group-level  
202 analysis included an additional covariate for the dataset to account for potential global signal  
203 differences between studies.

204 **2.8.1 Post-training effects: Correlation with DORT in veridical and inverted feedback group**

205 The first question of this study asked whether the individual degree of successful neurofeedback  
206 transfer is associated with individual differences in the cognitive control network. To answer this  
207 question, we conducted a general linear model (GLM) on the single subject level including one block-  
208 wise regressor for the IMAGINE\_REWARD condition and one for the REST condition with 190 timesteps  
209 (each condition comprised 9 onsets and lasted 20 s) for each of the four runs separately. Additionally,  
210 we modelled the first 5 TRs of every run as nuisance regressor and added also motion and physiological  
211 artefact regressors (see 2.7) in the design matrix. In total the GLM consisted of fifteen regressors. We  
212 formed the contrast IMAGINE\_REWARD-REST and compared it between Transfer and Baseline runs,  
213 i.e.  $(\text{IMAGINE\_REWARD-REST})_{\text{Transfer}} - (\text{IMAGINE\_REWARD-REST})_{\text{Baseline}}$ . At the group level, we tested  
214 for correlation of DORT with this contrast in a one-sample t-test. We ran these analyses separately for  
215 both the veridical and inverted feedback groups. To test for common and separate activity between  
216 the groups, we performed conjunction and disjunction analyses over the two group maps. Additionally,  
217 we performed a two-sample t-test group comparison analysis to identify significant group differences.

218 To identify activity within the cognitive control network, we used a cognitive control template based  
219 on the coordinates from a meta-analysis (Niendam et al., 2012). We created this template with  
220 fslmaths and spheres of 15 mm around all coordinates from the meta-analysis. In table S1 we identify  
221 regions of the cognitive control network where transfer success correlates with DORT both within the  
222 template. For statistical maps, we used FWE-corrected cluster level threshold with  $p < .05$  (cluster  
223 extent of 230 voxel) based on whole brain statistics  $p < .001$ . In addition, to test the functional  
224 specificity of our results, we performed a meta-analytic functional decoding analysis using the  
225 Neurosynth database ([www.neurosynth.org](http://www.neurosynth.org)). This relates the neural signatures of the cognitive control  
226 decoding network to other task-related neural patterns (Fig. S2).

227 2.8.2 Prediction error coding analysis during NF training

228 The second question of the study was to investigate whether successful neurofeedback performance  
229 was associated with a reduction in prediction error as assumed by a classic reinforcement learning  
230 mechanism. To address this issue specifically for the neurofeedback training runs we constructed a  
231 GLM that replaced the block (IMAGINE\_REWARD and REST) regressors with corresponding event  
232 regressors that modelled every TR and that we parametrically modulated with a time-resolved  
233 continuous prediction error (PE) term. This PE term was defined as difference between the current and  
234 the previous TR within the SN/VTA mask, i.e. (BOLD\_SN/VTA<sub>t</sub> - BOLD\_SN/VTA<sub>t-1</sub>); accordingly, in the  
235 upregulation condition the parametric modulator corresponded to IMAGINE\_REWARD<sub>t</sub> -  
236 IMAGINE\_REWARD<sub>t-1</sub>). To investigate if the prediction error decreases over time, we used the  
237 difference (parametric modulator PE (run 2) - parametric modulator PE (run 1), i.e. PE coding in  
238 neurofeedback training run 2 minus neurofeedback training run 1 (Figure 1A). This difference should  
239 become negative as prediction errors decrease with learning. On the group level, we correlated this  
240 contrast (difference in PE coding run2 - PE coding run1) with the DORT measure in a one-sample t-test  
241 to test for associations between a decrease in prediction error coding and successful self-regulation.

242 The results of this analysis, showing prediction error coding in the dorsolateral prefrontal  
243 cortex (dIPFC), inspired a functional connectivity analysis. Specifically, we investigated the functional

244 impact of the dlPFC prediction error signal on the SN/VTA using a psychophysiological interaction  
245 analysis using the gPPI v13 Toolbox (McLaren et al., 2012) based on the MNI coordinate of dlPFC (x=40,  
246 y=10, z=38) with a 5 mm sphere as seed region. We added activity from this seed region as  
247 physiological regressor to the original GLM (2.7.2) and interacted it with both the IMAGINE\_REWARD  
248 and REST regressors to form interaction regressors. Functional connectivity was calculated by  
249 contrasting the interaction terms IMAGINE\_REWARD-REST between second and first neurofeedback  
250 training run. We then correlated this contrast with DORT. The results were masked with the SN/VTA  
251 mask for illustration purposes. For statistical maps, we used a whole-brain threshold of  $p < .001$  (50  
252 voxel extent).

#### 253 2.8.3 Relation between DORT and reward sensitivity in the MID Task

254 To address the third aim of the study, we investigated the relationship between reward processing in  
255 the MID task and the capacity to successfully regulate the SN/VTA in the neurofeedback experiment.  
256 In particular, we considered two contrasts in the MID task (1) general reward sensitivity, defined as  
257 the sum of parametric modulators: small plus large reward (2) adaptive reward coding, defined as the  
258 difference between parametric modulators: small minus large reward. Again, we used correlation  
259 analysis at the group level to determine whether these two contrasts are related with individual  
260 transfer success (DORT) in the neurofeedback task. Moreover, to assess the commonalities of the  
261 neural activities in these different tasks, we performed a conjunction analysis of contrasts (1), (2) and  
262 the correlation of transfer-activity with DORT (see 2.8.1). For illustration purposes of this conjunction  
263 analysis, we used a threshold of  $p < .005$ , for reporting we used  $p < .001$  (cluster extent = 50).

264

#### 265 **2.9 Additional behavioral measurements**

266 **Strategies:** All participants were introduced to five example strategies (see 2.3) that might be used to  
267 up-regulate brain activity but also free to use their own strategies. At the end of the experiment,  
268 participants filled in a custom-made questionnaire on the strategies they used. To compare strategies

269 between the groups, we used a  $\chi^2$ -test to assess differences in the distribution of strategy usage. We  
270 did not observe any significant group differences in strategy use ( $p = .9$ ), and therefore did not consider  
271 this measurement in any further analysis.

272 **Personality measures:** To investigate whether individual differences in behavior and personality were  
273 associated with individual differences in DORT, Study 2 measured: (1) Smoking status in number of  
274 cigarettes per day; (2) verbal IQ as determined by the Multiple Word Test (MWT, Lehrl, 2005); (3)  
275 Positive and Negative Affect Score (PANAS) in the German version (Krohne et al., 1996); (4) attentional  
276 and nonplanning subscores of the Barratt Impulsivity Scale in the German version (Preuss et al., 2008).  
277 We tested for correlations with the DORT parameter using Pearson correlations. As none of these  
278 variables correlated significantly with the DORT parameter (all  $p > .5$ ), we did not consider them  
279 further.

## 280 **3 Results**

### 281 **3.1 No difference in degree of regulation transfer (DORT) across groups**

282 We first evaluated the DORT measure and compared it between the three datasets. There were no  
283 significant differences across all three groups (mean veridical group Study 1 = .01, mean veridical group  
284 Study 2 = -.02, mean inverted group Study 1 = -.05;  $F(2, 56) = .13$ ; Fig. 1). Moreover, also the direct  
285 comparison between the two veridical groups was not significant ( $T(39) = -.26, p = .8$ ). Accordingly, we  
286 combined the two veridical groups for subsequent analyses. Importantly, our participants showed  
287 considerable variation in DORT, which allowed us to investigate the individual differences in brain  
288 activity accompanying more or less successful regulation of the SN/VTA through neurofeedback. Thus,

289 the groups showed similar mean levels and considerable individual differences in self-regulation  
290 success.

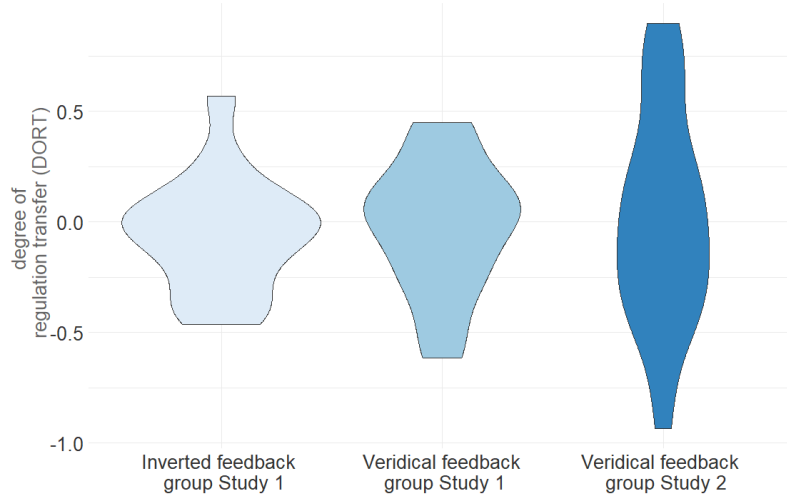


Figure 2 **Distribution of DORT across groups.** The DORT measure was distributed similarly in both groups receiving veridical feedback in Studies 1 and 2 and the control group receiving inverted feedback in Study 1. Accordingly, we found no evidence supporting a main effect of feedback on transfer. However, DORT varied substantially across individuals, which motivated the analyses using the individual self-regulation

291 **3.2 Individual variation in transfer: DORT associated with cognitive control network in  
292 veridical and amygdala activity in inverted feedback group**

293 **3.2.1 Veridical feedback group**

294 We investigated whether individual levels of successful SN/VTA self-regulation (DORT) were associated  
295 with increased post-training activity compared to pre-training activity ( $\text{IMAGINE\_REWARD-REST}_{\text{Transfer}}$   
296 –  $\text{IMAGINE\_REWARD-REST}_{\text{Baseline}}$ ). This analysis revealed several areas consistently reported by  
297 neurofeedback studies (see Fig. 2 in the meta-analysis of Sitaram et al., 2016), including dorsolateral  
298 prefrontal cortex (dlPFC), anterior cingulate cortex (ACC), lateral occipital cortex (LOC), and thalamus  
299 (Figure 3A and Table 1). To formally test for a more general association with the cognitive control  
300 network, we applied a cognitive control network template from a meta-analysis (Niendam et al., 2012),  
301 which in addition revealed neural activity in precuneus and striatum (Fig. 3B for exemplary illustrations

302 of dIPFC, ACC, temporal gyrus, and thalamus activity; Table S1 for full overview). Thus, regions of the  
 303 cognitive control network showed transfer to the extent that neurofeedback training of the  
 304 dopaminergic midbrain was successful.

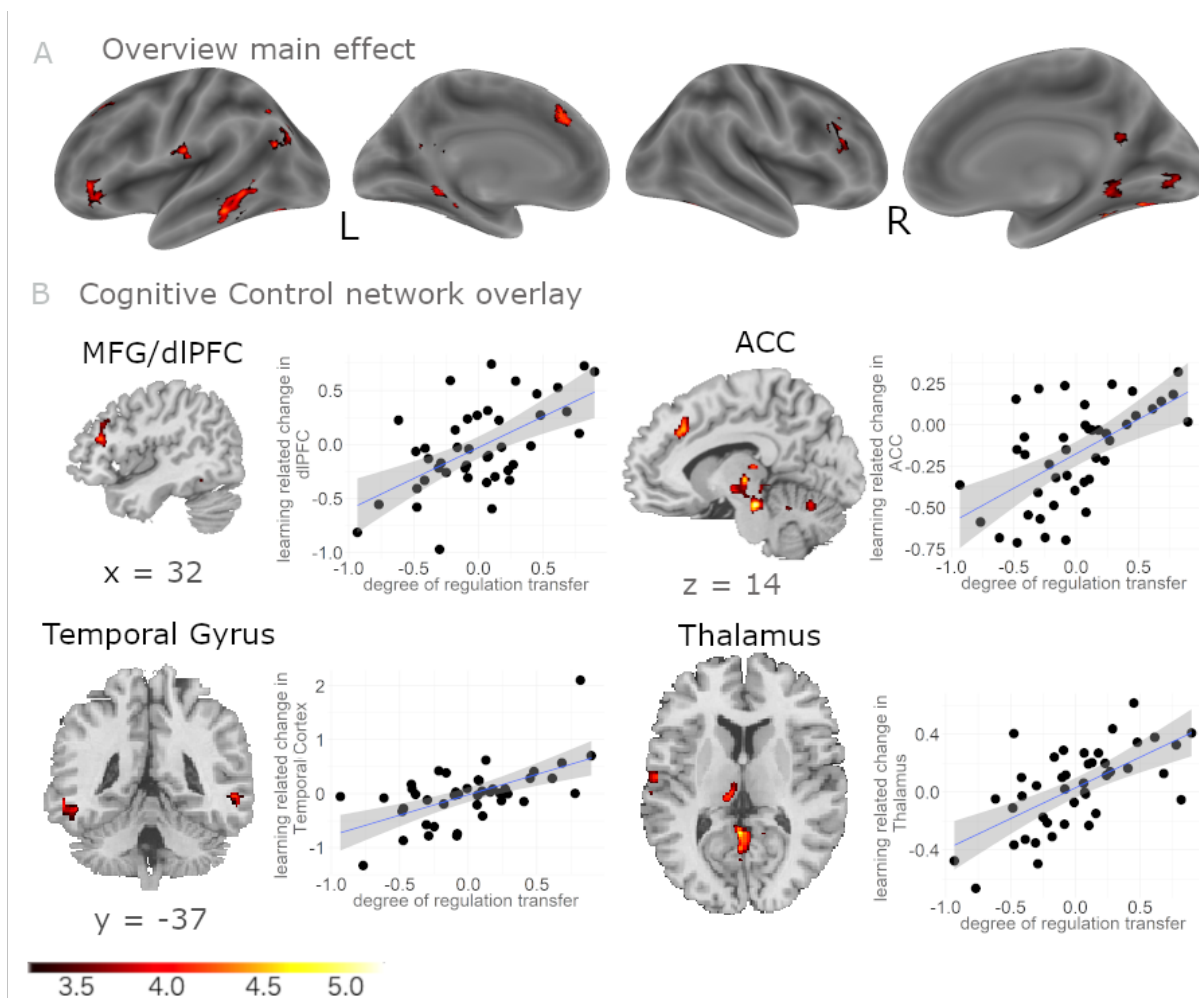


**Figure 3: Correlation of DORT with transfer success after training in verbal feedback group:** To investigate whole-brain neural activity correlating with successful SN/VTA self-regulation, we used DORT as measure of regulation success and correlated it with the contrast  $(\text{IMAGINE\_REWARD}_{\text{transfer}} - \text{REST}_{\text{transfer}}) - (\text{IMAGINE\_REWARD}_{\text{baseline}} - \text{REST}_{\text{baseline}})$  as measure of learning related change in neural activity. A) The analysis revealed task-specific correlations primarily within the cognitive control network (whole brain overview FWE-corrected with  $p < .05$  on cluster level, projected to lateral and medial sagittal sections). B) Exemplary correlations within the cognitive control network have been depicted, here in MFG/dIPFC, ACC, Thalamus, and bilateral Temporal Gyrus, to illustrate the association between neural activity with DORT. The correlations are for illustration purposes only without further significance testing to avoid double dipping. The grey shaded area identifies 95 % confidence interval.

MNI Coordinates						
Region Label	# voxels	t-value	x	y	z	
Cingulate Gyrus, posterior division	895	6.104	-3	-49	7	
Middle Frontal Gyrus (dorsolateral prefrontal cortex)	295	4.609	45	31	19	
Left Thalamus	1281	4.472	-9	-24	10	
Temporal Occipital Fusiform Cortex	715	5.858	32	-46	-22	

Lingual Gyrus (Right Parahippocampal Gyrus)	715	3.725	20	-46	-6
Right Cerebral White Matter (Right Hippocampus)	298	5.300	20	-18	-10
Left Hippocampus	408	3.703	-26	-33	-12
Left Cerebral White Matter (Left Middle Occipital Gyrus)	693	5.056	-36	-73	31
Left Cerebral White Matter (Left Superior Medial Gyrus, Anterior Cingulate Cortex)	579	4.960	-9	28	38
Intracalcarine Cortex (Right Lingual Gyrus)	856	4.048	6	-82	1
Occipital Fusiform Gyrus	474	4.928	29	-66	-12
Middle Temporal Gyrus (Left Inferior Temporal Gyrus)	1028	4.913	-62	-37	-16
Middle Temporal Gyrus (Left Inferior Temporal Gyrus)	1028	4.315	-59	-57	-3
Occipital Fusiform Gyrus	658	4.866	-42	-70	-19
Temporal Fusiform Cortex, posterior division	658	4.638	-39	-43	-28
Temporal Occipital Fusiform Cortex	658	4.401	-23	-66	-19
Superior Frontal Gyrus	310	4.736	6	2	80
Central Opercular Cortex (Left Superior Temporal Gyrus)	309	4.636	-59	-16	16
Left Cerebral White Matter (Left inferior Frontal Gyrus)	401	4.589	-39	35	-9
Location not in atlas	408	4.578	-14	-49	-22
Location not in atlas (Right Paracentral Lobule)	341	5.003	2	-39	82
Location not in atlas (Left Cerebellum IV)	856	4.947	-6	-66	-15

Table 1 Correlation of transfer activity ( $\text{IMAGINE\_REWARD}_{\text{transfer}} - \text{REST}_{\text{transfer}}$ ) - ( $\text{IMAGINE\_REWARD}_{\text{baseline}} - \text{REST}_{\text{baseline}}$ ) with DORT in veridical feedback group (see Figure 3a). Table shows all local maxima separated by more than 20 mm; for all clusters,  $p < 0.05$  FWE-corrected on cluster level,  $t > 3.30$ ;  $p < 0.001$ ;  $df = 40$ . Regions were labelled using the Harvard-Oxford atlas and/or the Anatomy Toolbox in parentheses; the activity in SN/VTA has been excluded from the table to avoid circularity;  $x, y, z$  = Montreal Neurological Institute (MNI) coordinates in the left-right, anterior-posterior, and inferior-superior dimensions, respectively.

305 3.2.2 Inverted feedback group

306 For the inverted feedback group, the same analysis resulted in partly distinct activations. In contrast  
 307 to the veridical feedback group, left amygdala activity correlated significantly with DORT (Fig. 4 and  
 308 Table S2). Importantly, activity in cognitive control areas reported above, such as dlPFC and ACC, was  
 309 significantly weaker in inverted than veridical feedback groups (Table S3 for disjunction and direct  
 310 statistical comparison). These regions therefore appear to play a preferential role for successful  
 311 transfer of SN/VTA self-regulation.

312 We also tested for common activity in the two feedback groups using conjunction analysis.  
313 Similar to the veridical group, the inverted feedback group showed correlations between DORT and  
314 activity in the precuneus, middle temporal gyrus, insula, IFG, thalamus, and parahippocampal gyrus  
315 (Table S4). These common areas appear to reflect non-specific regulation activity and may be  
316 associated with memory and introspection processes.

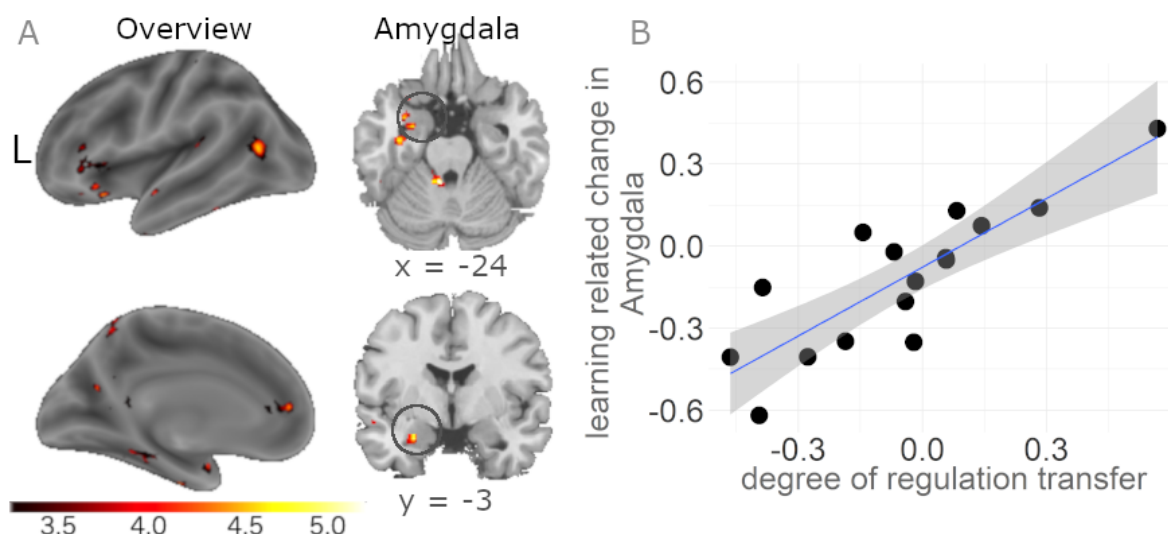


Figure 4 **Correlation of DORT with transfer success after training in inverted feedback group:** (A) Receiving inverted feedback resulted in a correlation between DORT as measure of regulation success and the contrast  $(\text{IMAGINE\_REWARD}_{\text{transfer}} - \text{REST}_{\text{transfer}}) - (\text{IMAGINE\_REWARD}_{\text{baseline}} - \text{REST}_{\text{baseline}})$  as measure of learning related change in the amygdala ( $p < .001$ ). This region was not observed in the veridical group. (B) The correlation depicts the positive association of neural activity in the amygdala with DORT. The plot is for illustration purposes only without further significance testing to avoid double dipping. The grey shaded area identifies the 95 % confidence interval.

317 **3.3 Reinforcement learning: DLPFC prediction error coding during neurofeedback training**  
318 **correlates with DORT**

319 To investigate whether reinforcement learning mechanisms contribute to successful neurofeedback  
320 transfer, we tested for time-resolved parametric prediction error related activity during the training  
321 runs. We reasoned that prediction error activity should decrease from early to late phases of  
322 neurofeedback training for successful regulators. At any time during neurofeedback training,  
323 participants needed to come up with their own predictions of the upcoming feedback signal and  
324 compare the predictions with actual feedback at the next time point. Similarly, in temporal difference  
325 learning models, prediction errors are calculated at each moment in time (Sutton and Barto, 2018).  
326 Therefore, we operationalized prediction error by subtracting the immediately preceding SN/VTA  
327 activity (prediction) from the present SN/VTA activity (outcome). This analysis revealed that prediction

328 error signals in dlPFC decreased with ongoing neurofeedback training only for participants with high  
329 DORT (Fig. 5). To assess this finding in more detail, we also analysed the two neurofeedback training  
330 runs separately. This analysis confirmed that more successful participants showed more pronounced  
331 dlPFC coding of prediction error in early compared to later training (see Fig. S3 for run-wise PE coding  
332 in dlPFC).

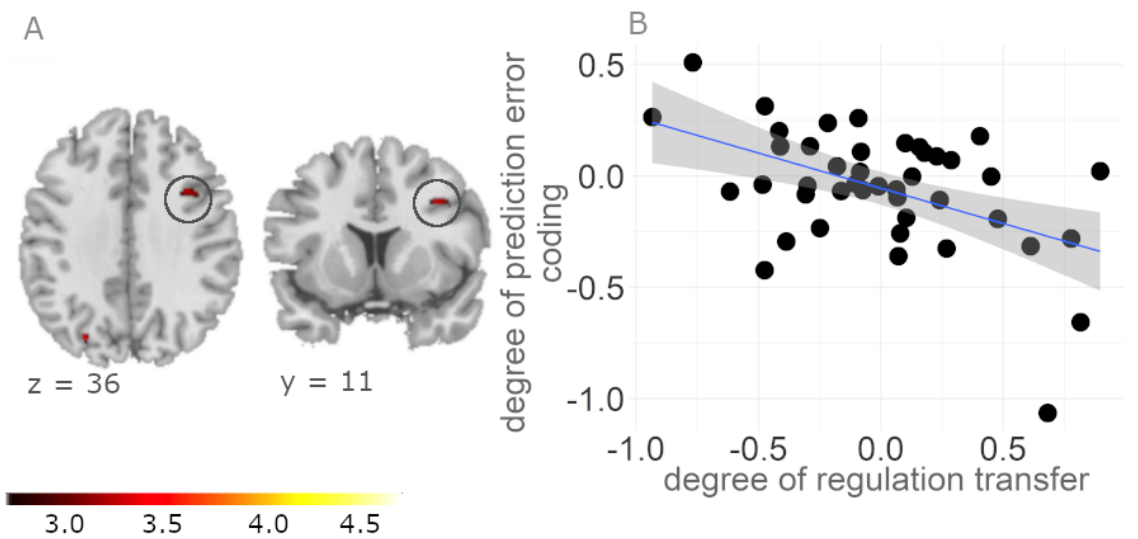


Figure 5: **Prediction error coding in dlPFC decreases during NF training in participants with successful SN/VTA self-regulation:** (A) The time-resolved neural prediction error signal, corresponding to the parametric difference between the current and immediately preceding feedback activity from the SN/VTA decreased with ongoing feedback training within dlPFC as a function of degree of regulation transfer ( $p < .001$ ). This finding is consistent with reinforcement learning theories, according to which prediction errors decrease as learning progresses. By extension, reinforcement learning mechanisms can explain successful neurofeedback training. (B) The plot depicts correlation of neural activity in the dlPFC with DORT. The plot is for illustration purposes only without further significance testing to avoid double dipping. The grey shaded area identifies the 95 % confidence interval.

### 333 3.4 Learning-related functional coupling of DLPFC with SN/VTA

334 Our finding of time-resolved prediction error coding in dlPFC inspired a complementary functional  
335 connectivity analysis. We used the prediction error coding area within the dlPFC as a seed region to  
336 investigate coupling to the SN/VTA region our participants aimed to regulate. Functional connectivity  
337 between the two regions increased with transfer success (Fig. 6; ( $t(40) = 3.79$ , cluster extent = 16, MNI  
338  $x = -2, y = -16, z = -15$ ). In other words, DORT and dlPFC to SN/VTA connectivity correlated positively.  
339 Note that this correlation of DORT with dlPFC-SN/VTA connectivity was task-related as it was enhanced  
340 during IMAGINE\_REWARD relative to REST (which served as psychological regressor) and independent  
341 of SN/VTA activity.

342

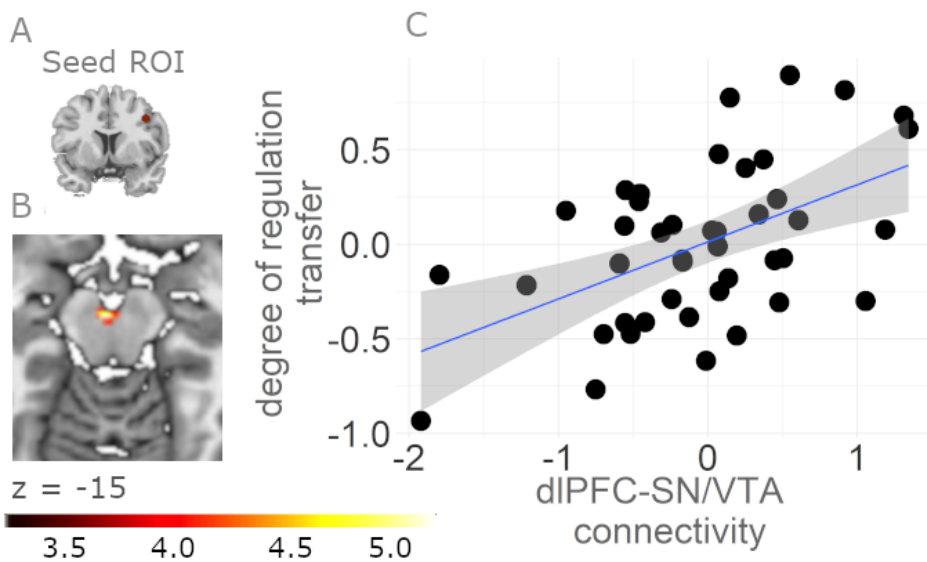


Figure 6 **Functional connectivity between dIPFC and SN/VTA correlates with transfer success:** (A) A functional connectivity analysis based on the prediction error coding seed region in the dIPFC (MNI coordinate 40, 10, 38, 5 cm sphere) revealed that increasing connectivity to the SN/VTA correlated with increasing success of neurofeedback training ( $p < .001$ ). (B) DORT increased with increasing connectivity between dIPFC and SN/VTA during IMAGINE\_REWARD vs. REST in neurofeedback training runs. Thus, dIPFC appears to regulate SN/VTA in proportion to the degree to which neurofeedback training is successful. (C) The correlation plot depicts connectivity between dIPFC and SN/VTA with DORT. The plot is for illustration purposes only without further significance testing to avoid double dipping. The grey shaded area identifies the 95 % confidence interval.

343 **3.5 Individual differences in dIPFC reward sensitivity during MID task correlate with**  
344 **regulation success**

345 In Study 2 we used the MID task to independently measure reward sensitivity and the capability to  
346 adapt to different reward contexts (Kirschner et al., 2018a). We asked whether individual measures of  
347 reward processing (measured with parametric and adaptive coding of reward related BOLD activity)  
348 are predictive for individual regulation. Specifically, we tested for correlations between DORT and MID  
349 reward sensitivity (sum of small and large reward parametric modulators) and MID adaptive reward  
350 coding (difference of small minus large reward parametric modulators). A conjunction of three  
351 correlations with DORT – reward sensitivity in the MID task, adaptive reward coding in the MID task  
352 and the contrast ( $\text{IMAGINE\_REWARD}_{\text{transfer}} - \text{REST}_{\text{transfer}}$ ) - ( $\text{IMAGINE\_REWARD}_{\text{baseline}} - \text{REST}_{\text{baseline}}$ ) outside  
353 SN/VTA revealed common neural activity in the dIPFC (center at MNI  $x = 40, y = 10, z = 38$ ; Fig. 7 and  
354 Table S6). Thus, the more successful individuals were at self-regulating SN/VTA as a result of

355 neurofeedback training, the more sensitive they were to reward and the more strongly they adapted  
356 to different reward contexts in the MID task.

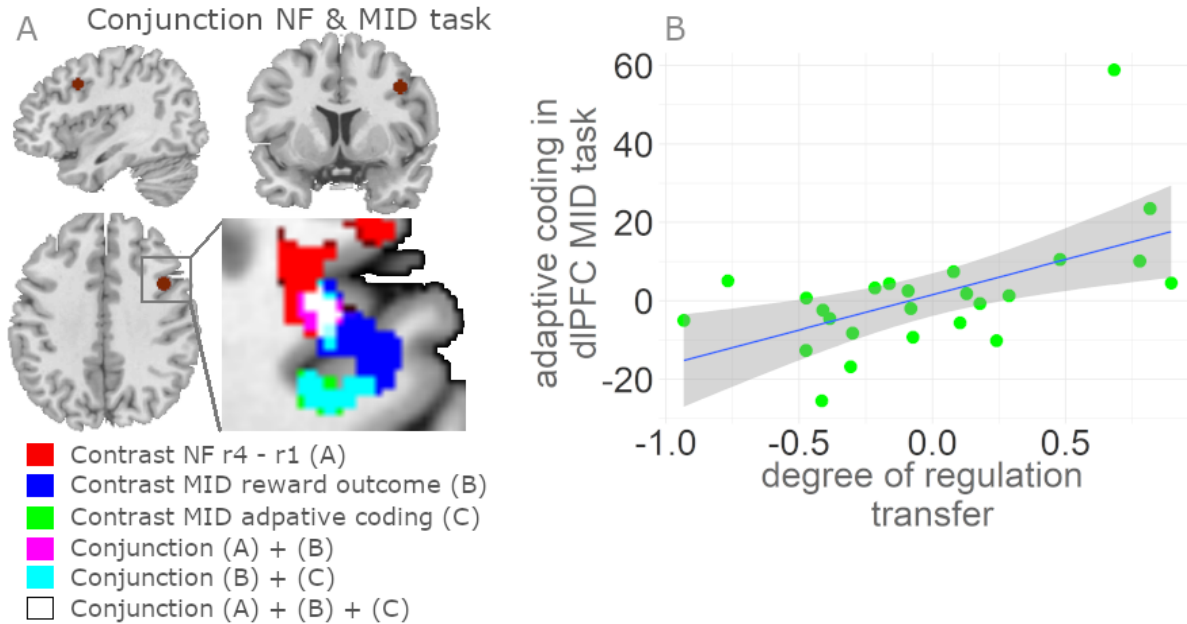


Figure 7 **Reward-sensitivity in dlPFC correlates with successful SN/VTA self-regulation:** (A) SN/VTA DORT in the neurofeedback task correlated with prefrontal reward sensitivity and adaptive coding in the MID task. A conjunction analysis around the peak coordinate in dlPFC showing prediction error coding during neurofeedback training (MNI x = 40, y = 10, z = 38, left) revealed common neural activity reflecting transfer ( $\text{IMAGINE\_REWARD}_{\text{transfer}} - \text{REST}_{\text{transfer}}$ ) - ( $\text{IMAGINE\_REWARD}_{\text{baseline}} - \text{REST}_{\text{baseline}}$ ) and reward sensitivity (small + large reward magnitude parametric modulators in MID, all contrasts with  $p < .001$ ). Moreover, individuals with more successful self-regulation of the SN/VTA showed stronger adaptive coding (which reflects higher sensitivity to small relative to large rewards) in the same region that also showed learning-related decreases in prediction error coding during neurofeedback training (right). (B) The correlation plot depicts the adaptive coding activity in dlPFC with DORT. The plot is for illustration purposes only without further significance testing to avoid double dipping. The grey shaded area identifies the 95 % confidence interval.

## 357 4 Discussion

358 In the present work, we used data acquired from two previous rt-fMRI neurofeedback studies to  
359 characterize individual differences and mechanisms in successfully transferred self-regulation of the  
360 dopaminergic midbrain after neurofeedback training. We found a strong relation between self-  
361 regulation success and increases in post-training activity in the cognitive control network. Moreover,  
362 we found four correlations with increasing transfer effects: (i) decreasing dlPFC prediction error signals  
363 during neurofeedback training, (ii) increasing connectivity of dlPFC to the SN/VTA for reward  
364 imagination compared to rest during transfer, (iii) increasing reward sensitivity in dlPFC and (iv)  
365 increasing adaptive reward coding in dlPFC in the independent MID task. Together, our study

366 elucidates the mechanistic control of the dopaminergic midbrain via the cognitive control network and  
367 suggests that reinforcement learning contributes to successful neurofeedback training.

368 Sustained self-regulation skills and the generalization of learning after neurofeedback training are key  
369 elements for practical applications and remain one of the major challenges in rt-FMRI neurofeedback  
370 research (Sulzer et al., 2013a). Results from previous neurofeedback studies of the reward system have  
371 been inconclusive (Greer et al., 2014; Kirschner et al., 2017; Sulzer et al., 2013b) and only one study  
372 (MacInnes et al., 2016) reported significant post-training activity in the VTA, and increased mesolimbic  
373 network connectivity. Methodological limitations might have hampered the ability to detect transfer  
374 effects. First, previous studies focused exclusively on self-regulation of one *a priori* target region, such  
375 as SN/VTA, instead of investigating large-scale post-training effects within the whole brain. Second,  
376 transfer effects were examined at the group-level, which did not reflect the individual learning success.  
377 In the present study we overcome both limitations by taking advantage of an individual measure of  
378 transfer success (DORT) and focusing on the whole brain.

379 One insight of the present study is that transfer success associates with neural activity in cognitive  
380 control network areas (Niendam et al., 2012; Parro et al., 2018), such as dlPFC and ACC. This network  
381 overlaps with regions that have been associated with feedback-related information processing during  
382 training (Marco-Pallarés et al., 2007, Emmert et al., 2016). Together, these findings suggest that the  
383 same regions contribute to acquisition and transfer of neurofeedback and that sustained post-training  
384 self-regulation generalizes across a functional network of different brain regions. Intriguingly, similar  
385 networks have been reported in skill learning. Future studies might investigate commonalities  
386 between neurofeedback and particularly cognitive skill learning, taking into account the specific  
387 temporal dynamics of both functions (Birbaumer et al., 2013; Tenison et al., 2016).

388 The finding that individuals with more successful regulation of the dopaminergic midbrain show  
389 stronger activation of cognitive control areas during transfer speaks to our understanding of how  
390 individual differences in cognitive control affect emotion regulation (Braver et al., 2010; Buhle et al.,

391 2014; Friedman and Miyake, 2017; Kohn et al., 2014). For example the working memory component  
392 of cognitive control has been shown to predict negative affect reduction through reappraisal and  
393 suppression (Hendricks and Buchanan, 2016) Interestingly, dopamine action (particularly at D1  
394 receptors) in dlPFC sustains working memory performance (Arnsten et al., 2015). Thus, it is conceivable  
395 that frontolimbic loops contribute to successful transfer.

396 Although speculative at this point, the positive post-training effects on the cognitive-control network  
397 activity might also have implications for transdiagnostic clinical applications. First, combining rt-fMRI  
398 neurofeedback training with different forms of psychotherapy such as cognitive behavioral therapy  
399 (Beck, 2005), dialectical behavioral therapy (Lynch et al., 2007), or psychodynamic therapy (Bateman  
400 and Fonagy, 2010; Have-de Labije and Neborsky, 2012; Maroda, 2010) could improve emotion  
401 regulation deficits prevalent in several psychiatric disorders including substance use disorders,  
402 depression, anxiety and personality disorders. With particular attention to substance use disorders,  
403 maladaptive changes in neuroplasticity within the cognitive control network are closely associated  
404 with loss of control and compulsive drug-seeking (George and Koob, 2010; Holmes et al., 2016; Koob  
405 and Volkow, 2010). In these patients, neurofeedback training might be able to directly target the  
406 biological correlates and reinstate function of the cognitive-control network.

407 We found stronger reductions in prediction error coding in the DLPFC for regulators than non-  
408 regulators. This finding suggests that prediction error-driven reinforcement learning was more  
409 pronounced in regulators than non-regulators and provides empirical evidence for previous theoretical  
410 proposals on the mechanisms of neurofeedback learning independent of feedback modality  
411 (Birbaumer et al., 2013). Thus, reinforcement learning mechanisms provide a framework for  
412 understanding how neurofeedback works. Future research may want to investigate whether the rich  
413 theoretical and empirical tradition of reinforcement learning, (e.g. Pearce, 2008), can be harnessed to  
414 facilitate neurofeedback training.

415 We found that successful SN/VTA self-regulation is associated with an increased functional coupling  
416 between dlPFC regions coding prediction error and the dopaminergic midbrain. This coupling fits well  
417 with anatomical connections between dlPFC and the dopaminergic midbrain (Frankle et al., 2006;  
418 Sesack et al., 2003) as well as functional connectivity studies on motivation (Ballard et al., 2011) and  
419 animal studies on prefrontal regulation of midbrain activity (Gao et al., 2007; Jo and Mizumori, 2016).  
420 The animal work suggests that prefrontal cortex controls dopaminergic neurons primarily indirectly,  
421 through inhibitory relay neurons. By showing top-down control of the midbrain, our data go beyond  
422 previous connectivity studies of the dopamine system, which primarily focused on coupling between  
423 the prefrontal cortex and the striatum (Chatham et al., 2014; Schenk et al., 2017; Weber et al., 2018).  
424 At the functional level, a recent study on creative problem solving in humans highlights that dlPFC is  
425 involved in experiencing a moment of insight, the so called Aha!-moment (Tik et al., 2018). According  
426 to this effective connectivity study, dlPFC could upregulate the VTA/SN via striatal connections during  
427 such a moment. On the other hand, in trials where no solution was found for a given problem, also no  
428 significant connectivity was observed. This study supports our finding that dlPFC-SN/VTA connectivity  
429 plays an important role in self-guided motivation and in internal reward processing. Our finding  
430 highlights that cognitive and affective mechanisms associated with different experiences also involve  
431 different neural pathways. Future studies should investigate to what degree individual differences in  
432 the functional architecture of brain networks (Hahn et al., 2014) influence these internal reward  
433 mechanisms and to which degree different strategies can influence neurofeedback training success.  
434 Our independent reward task revealed that individual differences in prefrontal reward sensitivity and  
435 efficient adaptive reward coding were associated with successful SN/VTA self-regulation. Adaptive  
436 coding of rewards captures the notion that neural activity (output) should match the most likely inputs  
437 to maximize efficiency and representational precision (Wark et al., 2007). Accordingly, we previously  
438 showed that reward regions encode a small range of rewards more strongly than the large range of  
439 rewards (Kirschner et al., 2018a, 2016). Interestingly, participants who were more sensitive to small  
440 rewards were also more successful in self-regulation of the dopaminergic midbrain in the present

441 study. When participants in a typical neurofeedback training paradigm succeed at increasing the  
442 activity of the self-regulated area, the ensuing change in visual stimulation (positive neurofeedback)  
443 may constitute a small reward. By extension, adaptive reward coding may therefore provide a useful  
444 handle on identifying regulators. Moreover, future neurofeedback experiments should consider  
445 scaling the feedback signal to avoid sensitivity limitations, particularly in individuals with reduced  
446 adaptive coding.

447 A potential limitation of our study is that we used a combined mask for SN and VTA even though  
448 differences in functionality and anatomy have been reported for the two regions (reviewed e.g. in  
449 Trutti et al., 2019), with the SN more related to motor functions and the VTA to reward functions.  
450 However, it should be kept in mind that when viewed through the lens of recording and imaging rather  
451 than lesion techniques the differences are more gradual than categorical (Düzel et al., 2009). Still,  
452 future studies may want to use more specific feedback from one or the other region to more  
453 specifically target potential differences in functions.

## 454 **5 Conclusions**

455 We showed that successful transfer in SN/VTA self-regulation after neurofeedback training is  
456 associated with activity in the cognitive control network and dlPFC. Future studies could employ  
457 cognitive control activity during neurofeedback training to boost success rates and clinical outcomes.  
458 Furthermore, our findings of decreasing prediction error signals in dlPFC suggest that associative  
459 learning contributes to real-time fMRI neurofeedback effects. Finally, we show that higher individual  
460 reward sensitivity increases the chance of neurofeedback training success. Patients with reduced  
461 reward sensitivity may therefore benefit from careful scaling of the neurofeedback information.

## Acknowledgments

The authors would like to thank Silvia Maier and Stephan Nebe for comments on previous versions of the manuscript and fruitful discussions.

This project was supported by the European Union's Horizon 2020 research and innovation program under the Grant Agreement No 794395 (to LH) and grant 100014\_165884 from the Swiss National Science Foundation (to PT). MK received grant support from the National Bank Fellowship (McGill) and Swiss National Science Foundation (P2SKP3\_178175).

The authors declare no competing financial interests.

## References

Alkoby, O., Abu-Rmileh, A., Shriki, O., Todder, D., 2018. Can We Predict Who Will Respond to Neurofeedback? A Review of the Inefficacy Problem and Existing Predictors for Successful EEG Neurofeedback Learning. *Neuroscience* 378, 155–164. <https://doi.org/10.1016/J.NEUROSCIENCE.2016.12.050>

Arnsten, A.F.T., Wang, M., Paspalas, C.D., 2015. Dopamine's Actions in Primate Prefrontal Cortex: Challenges for Treating Cognitive Disorders. *Pharmacol. Rev.* 67, 681–696. <https://doi.org/10.1124/pr.115.010512>

Ballard, I.C., Murty, V.P., Carter, R.M., MacInnes, J.J., Huettel, S.A., Adcock, R.A., 2011. Dorsolateral Prefrontal Cortex Drives Mesolimbic Dopaminergic Regions to Initiate Motivated Behavior. *J. Neurosci.* 31, 10340–10346. <https://doi.org/10.1523/jneurosci.0895-11.2011>

Bateman, A., Fonagy, P., 2010. Mentalization based treatment for borderline personality disorder. *World Psychiatry* 9, 11–5.

Beck, A.T., 2005. The current state of cognitive therapy: A 40-year retrospective. *Arch. Gen. Psychiatry*. <https://doi.org/10.1001/archpsyc.62.9.953>

Birbaumer, N., Ruiz, S., Sitaram, R., 2013. Learned regulation of brain metabolism. *Trends Cogn. Sci.* 17, 295–302. <https://doi.org/10.1016/j.tics.2013.04.009>

Braver, T.S., Cole, M.W., Yarkoni, T., 2010. Vive les differences! Individual variation in neural mechanisms of executive control. *Curr. Opin. Neurobiol.* <https://doi.org/10.1016/j.conb.2010.03.002>

Bromberg-Martin, E.S., Matsumoto, M., Hikosaka, O., 2010. Dopamine in Motivational Control: Rewarding, Aversive, and Alerting. *Neuron*. <https://doi.org/10.1016/j.neuron.2010.11.022>

Buhle, J.T., Silvers, J.A., Wage, T.D., Lopez, R., Onyemekwu, C., Kober, H., Webe, J., Ochsner, K.N., 2014. Cognitive reappraisal of emotion: A meta-analysis of human neuroimaging studies. *Cereb. Cortex* 24, 2981–2990. <https://doi.org/10.1093/cercor/bht154>

Burke, C.J., Tobler, P.N., 2016. Time, Not Size, Matters for Striatal Reward Predictions to Dopamine. *Neuron*. <https://doi.org/10.1016/j.neuron.2016.06.029>

Chatham, C.H., Frank, M.J., Badre, D., 2014. Corticostriatal output gating during selection from working memory. *Neuron* 81, 930–942. <https://doi.org/10.1016/j.neuron.2014.01.002>

Deserno, L., Schlagenhauf, F., Heinz, A., 2016. Striatal dopamine, reward, and decision making in schizophrenia. *Dialogues Clin. Neurosci.* 18, 77–89.

Düzel, E., Bunzeck, N., Guitart-Masip, M., Wittmann, B., Schott, B.H., Tobler, P.N., 2009. Functional imaging of the human dopaminergic midbrain. *Trends Neurosci.* 32, 321–328. <https://doi.org/10.1016/j.tins.2009.02.005>

Emmert, K., Kopel, R., Koush, Y., Maire, R., Senn, P., De Ville, D. Van, Haller, S., 2017. Continuous vs. intermittent neurofeedback to regulate auditory cortex activity of tinnitus patients using real-time fMRI - A pilot study. *NeuroImage Clin.* 14, 97–104. <https://doi.org/10.1016/j.nicl.2016.12.023>

Frankle, W.G., Laruelle, M., Haber, S.N., 2006. Prefrontal cortical projections to the midbrain in primates: Evidence for a sparse connection. *Neuropsychopharmacology* 31, 1627–1636.

<https://doi.org/10.1038/sj.npp.1300990>

Friedman, N.P., Miyake, A., 2017. Unity and diversity of executive functions: Individual differences as a window on cognitive structure. *Cortex*. <https://doi.org/10.1016/j.cortex.2016.04.023>

Friston, K., Schwartenbeck, P., FitzGerald, T., Moutoussis, M., Behrens, T., Dolan, R.J., 2014. The anatomy of choice: Dopamine and decision-making. *Philos. Trans. R. Soc. B Biol. Sci.* 369. <https://doi.org/10.1098/rstb.2013.0481>

Gao, M., Liu, C.-L., Yang, S., Jin, G.-Z., Bunney, B.S., Shi, W.-X., 2007. Functional Coupling between the Prefrontal Cortex and Dopamine Neurons in the Ventral Tegmental Area. *J. Neurosci.* 27, 5414–5421. <https://doi.org/10.1523/jneurosci.5347-06.2007>

George, O., Koob, G.F., 2010. Individual differences in prefrontal cortex function and the transition from drug use to drug dependence. *Neurosci. Biobehav. Rev.* <https://doi.org/10.1016/j.neubiorev.2010.05.002>

Greer, S.M., Trujillo, A.J., Glover, G.H., Knutson, B., 2014. Control of nucleus accumbens activity with neurofeedback. *Neuroimage* 96, 237–244. <https://doi.org/10.1016/j.neuroimage.2014.03.073>

Hahn, A., Kranz, G.S., Sladky, R., Ganger, S., Windischberger, C., Kasper, S., Lanzenberger, R., 2014. Individual Diversity of Functional Brain Network Economy. *Brain Connect.* 5, 156–165. <https://doi.org/10.1089/brain.2014.0306>

Have-de Labije, J., Neborsky, R., 2012. Mastering intensive short-term dynamic psychotherapy: a roadmap to the unconscious. Karnac Books, London.

Hendricks, M.A., Buchanan, T.W., 2016. Individual differences in cognitive control processes and their relationship to emotion regulation. *Cogn. Emot.* 30, 912–924. <https://doi.org/10.1080/02699931.2015.1032893>

Holmes, A.J., Hollinshead, M.O., Roffman, J.L., Smoller, J.W., Buckner, R.L., 2016. Individual Differences in Cognitive Control Circuit Anatomy Link Sensation Seeking, Impulsivity, and Substance Use. *J. Neurosci.* 36, 4038–4049. <https://doi.org/10.1523/jneurosci.3206-15.2016>

Huys, Q.J.M., Tobler, P.N., Hasler, G., Flagel, S.B., 2014. The role of learning-related dopamine signals in addiction vulnerability, in: *Progress in Brain Research.* pp. 31–77. <https://doi.org/10.1016/B978-0-444-63425-2.00003-9>

Jo, Y.S., Mizumori, S.J., 2016. Prefrontal Regulation of Neuronal Activity in the Ventral Tegmental Area. *Cereb. Cortex* 26, 4057–4068. <https://doi.org/10.1093/cercor/bhv215>

Kirschner, M., Hager, O.M., Bischof, M., Hartmann, M.N., Kluge, A., Seifritz, E., Tobler, P.N., Kaiser, S., 2016. Ventral striatal hypoactivation is associated with apathy but not diminished expression in patients with schizophrenia. *J. Psychiatry Neurosci.* 41, 152–161. <https://doi.org/10.1503/jpn.140383>

Kirschner, M., Haugg, A., Manoliu, A., Simon, J.J., Huys, Q.J.M., Seifritz, E., Tobler, P.N., Kaiser, S., 2018a. Deficits in context-dependent adaptive coding in early psychosis and healthy individuals with schizotypal personality traits. *Brain* 141, 2806–2819. <https://doi.org/10.1093/brain/awy203>

Kirschner, M., Haugg, A., Manoliu, A., Simon, J.J., Huys, Q.J.M., Seifritz, E., Tobler, P.N., Kaiser, S., 2018b. Deficits in context-dependent adaptive coding in early psychosis and healthy individuals with schizotypal personality traits. *Brain* 141, 2806–2819. <https://doi.org/10.1093/brain/awy203>

Kirschner, M., Sladky, R., Haugg, A., Staempfli, P., Jehli, E., Hodel, M., Engeli, E., Hoesli, S., Baumgartner,

M.R., Sulzer, J., Huys, Q.J.M., Seifritz, E., Quednow, B.B., Scharnowski, F., Herdener, M., 2018c. Self-regulation of the Dopaminergic Reward Circuit in Cocaine Users with Mental Imagery and Neurofeedback. *bioRxiv*.

Kirschner, M., Stämpfli, P., Jehli, E., Hodel, M., Engeli, E., Hulka, L., Scharnowski, F., Sulzer, J., Seifritz, E., Quednow, B., Herdener, M., 2017. Self-regulation and real time fMRI neurofeedback of the dopaminergic reward system in cocaine users Background & Objectives Key findings. *Proc. Annu. Meet. Soc. Biol. Psychiatry* 8001.

Klein, M.O., Battagello, D.S., Cardoso, A.R., Hauser, D.N., Bittencourt, J.C., Correa, R.G., 2019. Dopamine: Functions, Signaling, and Association with Neurological Diseases. *Cell. Mol. Neurobiol.* 39, 31–59. <https://doi.org/10.1007/s10571-018-0632-3>

Kohn, N., Eickhoff, S.B., Scheller, M., Laird, A.R., Fox, P.T., Habel, U., 2014. Neural network of cognitive emotion regulation - An ALE meta-analysis and MACM analysis. *Neuroimage* 87, 345–355. <https://doi.org/10.1016/j.neuroimage.2013.11.001>

Koob, G.F., Volkow, N.D., 2010. Neurocircuitry of addiction. *Neuropsychopharmacology* 35, 217–38. <https://doi.org/10.1038/npp.2009.110>

Krohne, H.W., Egloff, B., Kohlmann, C.-W., Tausch, A., 1996. Untersuchung mit einer deutschen Form der Positive and Negative Affect Schedule (PANAS). *Diagnostica* 42, 139–156.

Lehrl, S., 2005. Mehrfachwahl-Wortschatz-Intelligenztest MWT-B., 5th ed. Spitta Verlag, Balingen.

Lynch, T.R., Trost, W.T., Salsman, N., Linehan, M.M., 2007. Dialectical Behavior Therapy for Borderline Personality Disorder. *Annu. Rev. Clin. Psychol.* 3, 181–205. <https://doi.org/10.1146/annurev.clinpsy.2.022305.095229>

MacInnes, J.J., Dickerson, K.C., Chen, N. kuei, Adcock, R.A., 2016. Cognitive Neurostimulation: Learning to Volitionally Sustain Ventral Tegmental Area Activation. *Neuron* 89, 1331–1342. <https://doi.org/10.1016/j.neuron.2016.02.002>

Maia, T. V., Frank, M.J., 2017. An Integrative Perspective on the Role of Dopamine in Schizophrenia. *Biol. Psychiatry* 81, 52–66. <https://doi.org/10.1016/j.biopsych.2016.05.021>

Marco-Pallarés, J., Müller, S.V., Münte, T.F., 2007. Learning by doing: An fMRI study of feedback-related brain activations. *Neuroreport* 18, 1423–1426. <https://doi.org/10.1097/WNR.0b013e3282e9a58c>

Maroda, K.J., 2010. Psychodynamic Techniques: Working with Emotion in the Therapeutic Relationship, *Journal of Phenomenological Psychology*. Guilford Press, New York, US. <https://doi.org/10.1163/156916211x567505>

McLaren, D.G., Ries, M.L., Xu, G., Johnson, S.C., 2012. A generalized form of context-dependent psychophysiological interactions (gPPI): A comparison to standard approaches. *Neuroimage* 61, 1277–1286. <https://doi.org/10.1016/j.neuroimage.2012.03.068>

Meder, D., Herz, D.M., Rowe, J.B., Lehéricy, S., Siebner, H.R., 2019. The role of dopamine in the brain - lessons learned from Parkinson's disease. *Neuroimage* 190, 79–93. <https://doi.org/10.1016/j.neuroimage.2018.11.021>

Miyapuram, K.P., Tobler, P.N., Gregorios-Pippas, L., Schultz, W., 2012. BOLD responses in reward regions to hypothetical and imaginary monetary rewards. *Neuroimage* 59, 1692–1699. <https://doi.org/10.1016/j.neuroimage.2011.09.029>

Murty, V.P., Shermohammed, M., Smith, D. V., Carter, R.M., Huettel, S.A., Adcock, R.A., 2014. Resting state networks distinguish human ventral tegmental area from substantia nigra. *Neuroimage* 100, 580–9. <https://doi.org/10.1016/j.neuroimage.2014.06.047>

Niendam, T.A., Laird, A.R., Ray, K.L., Dean, Y.M., Glahn, D.C., Carter, C.S., 2012. Meta-analytic evidence for a superordinate cognitive control network subserving diverse executive functions. *Cogn. Affect. Behav. Neurosci.* 12, 241–68. <https://doi.org/10.3758/s13415-011-0083-5>

Oblak, E.F., Lewis-Peacock, J.A., Sulzer, J.S., 2017. Self-regulation strategy, feedback timing and hemodynamic properties modulate learning in a simulated fMRI neurofeedback environment. *PLoS Comput. Biol.* 13, e1005681. <https://doi.org/10.1371/journal.pcbi.1005681>

Parro, C., Dixon, M.L., Christoff, K., 2018. The neural basis of motivational influences on cognitive control. *Hum. Brain Mapp.* 39, 5097–5111. <https://doi.org/10.1002/hbm.24348>

Pearce, J., 2008. *Animal Learning and Cognition: An Introduction*, 3rd ed.

Preuss, U.W., Rujescu, D., Giegling, I., Watzke, S., Koller, G., Zetsche, T., Meisenzahl, E.M., Soyka, M., Möller, H.J., 2008. Psychometrische evaluation der deutschsprachigen version der Barratt-Impulsiveness-Skala. *Nervenarzt* 79, 305–319. <https://doi.org/10.1007/s00115-007-2360-7>

Radua, J., Stoica, T., Scheinost, D., Pittenger, C., Hampson, M., 2018. Neural Correlates of Success and Failure Signals During Neurofeedback Learning. *Neuroscience* 378, 11–21. <https://doi.org/10.1016/j.neuroscience.2016.04.003>

Schenk, L.A., Sprenger, C., Onat, S., Colloca, L., Büchel, C., 2017. Suppression of Striatal Prediction Errors by the Prefrontal Cortex in Placebo Hypoalgesia. *J. Neurosci.* 37, 9715–9723. <https://doi.org/10.1523/jneurosci.1101-17.2017>

Schultz, W., 2016. Dopamine reward prediction error coding. *Dialogues Clin. Neurosci.* 18, 23–32.

Schultz, W., 1998. Predictive Reward Signal of Dopamine Neurons. *J. Neurophysiol.* 80, 1–27.

Sesack, S.R., Carr, D.B., Omelchenko, N., Pinto, A., 2003. Anatomical Substrates for Glutamate-Dopamine Interactions: Evidence for Specificity of Connections and Extrasynaptic Actions, in: *Annals of the New York Academy of Sciences*. John Wiley & Sons, Ltd (10.1111), pp. 36–52. <https://doi.org/10.1196/annals.1300.066>

Simon, J.J., Cordeiro, S.A., Weber, M.A., Friederich, H.C., Wolf, R.C., Weisbrod, M., Kaiser, S., 2015. Reward System Dysfunction as a Neural Substrate of Symptom Expression Across the General Population and Patients with Schizophrenia. *Schizophr. Bull.* 41, 1370–1378. <https://doi.org/10.1093/schbul/sbv067>

Sitaram, R., Ros, T., Stoeckel, L., Haller, S., Scharnowski, F., Lewis-Peacock, J., Weiskopf, N., Blefari, M.L., Rana, M., Oblak, E., Birbaumer, N., Sulzer, J., 2016. Closed-loop brain training: the science of neurofeedback. *Nat. Rev. Neurosci.* 18, 86–100. <https://doi.org/10.1038/nrn.2016.164>

Sladky, R., Baldinger, P., Kranz, G.S., Tröstl, J., Höfflich, A., Lanzenberger, R., Moser, E., Windischberger, C., 2013. High-resolution functional MRI of the human amygdala at 7 T. *Eur. J. Radiol.* 82, 728–733. <https://doi.org/10.1016/j.ejrad.2011.09.025>

Sladky, R., Friston, K.J., Tröstl, J., Cunnington, R., Moser, E., Windischberger, C., 2011. Slice-timing effects and their correction in functional MRI. *Neuroimage* 58, 588–594. <https://doi.org/10.1016/j.neuroimage.2011.06.078>

Spunt, B., 2016. Spunt/Bspmview: Bspmview V.20161108. <https://doi.org/10.5281/ZENODO.168074>

Sulzer, J., Haller, S., Scharnowski, F., Weiskopf, N., Birbaumer, N., Blefari, M.L., Bruehl, A.B., Cohen, L.G., DeCharms, R.C., Gassert, R., Goebel, R., Herwig, U., LaConte, S., Linden, D., Luft, A., Seifritz, E., Sitaram, R., 2013a. Real-time fMRI neurofeedback: Progress and challenges. *Neuroimage* 76, 386–399. <https://doi.org/10.1016/j.neuroimage.2013.03.033>

Sulzer, J., Sitaram, R., Blefari, M.L., Kollias, S., Birbaumer, N., Stephan, K.E., Luft, A., Gassert, R., 2013b. Neurofeedback-mediated self-regulation of the dopaminergic midbrain. *Neuroimage* 75, 176–184. <https://doi.org/10.1016/j.neuroimage.2013.02.041>

Sutton, R.S., Barto, A.G., 2018. Reinforcement Learning: An Introduction, 2nd ed. A Bradford Book, Cambridge.

Tenison, C., Fincham, J.M., Anderson, J.R., 2016. Phases of learning: How skill acquisition impacts cognitive processing. *Cogn. Psychol.* 87, 1–28. <https://doi.org/10.1016/J.COGPSYCH.2016.03.001>

Tik, M., Sladky, R., Luft, C.D.B., Willinger, D., Hoffmann, A., Banissy, M.J., Bhattacharya, J., Windischberger, C., 2018. Ultra-high-field fMRI insights on insight: Neural correlates of the Aha-moment. *Hum. Brain Mapp.* 39, 3241–3252. <https://doi.org/10.1002/hbm.24073>

Tobler, P.N., Fiorillo, C.D., Schultz, W., 2005. Adaptive coding of reward value by dopamine neurons. *Science* 307, 1642–5. <https://doi.org/10.1126/science.1105370>

Tobler, P.N., Fletcher, P.C., Bullmore, E.T., Schultz, W., 2007. Learning-Related Human Brain Activations Reflecting Individual Finances. *Neuron* 54, 167–175. <https://doi.org/10.1016/j.neuron.2007.03.004>

Trutti, A.C., Mulder, M.J., Hommel, B., Forstmann, B.U., 2019. Functional neuroanatomical review of the ventral tegmental area. *Neuroimage*. <https://doi.org/10.1016/j.neuroimage.2019.01.062>

Wark, B., Lundstrom, B.N., Fairhall, A., 2007. Sensory adaptation. *Curr. Opin. Neurobiol.* 17, 423–9. <https://doi.org/10.1016/j.conb.2007.07.001>

Weber, S.C., Kahnt, T., Quednow, B.B., Tobler, P.N., 2018. Frontostriatal pathways gate processing of behaviorally relevant reward dimensions. *PLoS Biol.* 16, e2005722. <https://doi.org/10.1371/journal.pbio.2005722>

Weissenbacher, A., Kasess, C., Gerstl, F., Lanzenberger, R., Moser, E., Windischberger, C., 2009. Correlations and anticorrelations in resting-state functional connectivity MRI: A quantitative comparison of preprocessing strategies. *Neuroimage* 47, 1408–1416. <https://doi.org/10.1016/j.neuroimage.2009.05.005>

Wise, R.A., 2004. Dopamine, learning and motivation. *Nat. Rev. Neurosci.* <https://doi.org/10.1038/nrn1406>

Wu, J., Gao, M., Shen, J.X., Shi, W.X., Oster, A.M., Gutkin, B.S., 2013. Cortical control of VTA function and influence on nicotine reward. *Biochem. Pharmacol.* <https://doi.org/10.1016/j.bcp.2013.07.013>